INTRODUCTION OF EMERGENT AND FISSION CLASSIFICATIONS TO PAIRED-OBJECT SYSTEMS FOR MORPHOLOGICAL TAXONOMY

Tarzan Graystone

Author affiliation

Autonomous Citizen Science Alliance

Abstract

The scope of this exercise is not to propose any initiation mechanism[1] for proband systems but rather to follow the latter components of an emergent system event and extrapolate a timeline, to connect the dots, in a lineage of multi-object systems from , primordial emergent anlage to a fission system. These taxonomic classifications will resolve multi-object morphological dilemmas. The next publication will include discussions of larger family groups.

Introduction

The results of fission events from a primordial anlage yields various of multi-object or paired-object systems into P1 ‘parents/proximals’ and C1 ‘children/closest.’[2] The “P1” of this system pairing is usually the larger object based upon size, chemistry, physical and kinetic properties. Moreover, an unary emergent precursor object theoretically splits into a multi-object system with two or more resulting independent objects. This report analyzes properties of those proximal and closest, data-driven fission paired-objects by redshift.

Data-driven system selection

Again, the scope of this exercise is neither to propose any initiation mechanism nor establish any generalities about a proband system but rather to follow the latter components of fission and extrapolate from paired-object systems back to an anlage. In Ernst Haeckel's aphorism, "ontogeny recapitulates phylogeny." The objects across redshifts z = 0.01 - 0.1 matched by the value of r(c1) - r(p1) or (rdif) show that these pairs do share a morphological 'family' resemblance. Paired-object systems from the analysis and supplemental pairs with their unprocessed records are included in the appendix. Analyzed herein are the putative binary pairings chosen from isolated pairs or the nearest data-driven pair of a multi-object family. These processes are delineated from within and across redshifts (looking for like-parings) and through analysis of their properties. The primordial emergent anlage system is easily likened to an irregular-type system usually with an obvious overlap of its ‘internal’ objects.

Historical overview

This study draws strength from many years of publications disproving or finding fault with the merger hypothesis. Fission terms have been around for some time. The terms “post-eruptive” (Zwicky 1971) and “fission” were used to describe “peculiar”[3]

non-merging systems. There are several synopses from NED Level5 which will be useful as a rich source of accounts that can be rewritten as fission papers in the future. Previously, papers concluded with puzzling outcomes and outright incongruous observations. Many reports gleaned their "merger" subset from a much larger multi-object population and those too should be reexamined along with their selected analysis samples.

Figure 1 SDSS Level 5 Classification type table. [4]

Galaxy Morphology:	**merger**
Description:	**Observed feature suggest a merging event (theory laden).**
Associated Classifications:	**5 associated classes Hide/Show**
Exact Classifications Count:	**6**
Associated Data Count:	**11 entries for 9 objects (retrieve objects)**
Associated Reference Codes:	**1981RSA...C...0000S 1982ESOU..C...0000L 1994CAG1..B...0000S 2011ApJ...733L..47F**

Although many objects from pairs have obvious morphological traits more will be added to the data after classifications become available. It should be noted that the initial emergent transformation can result in a variety of outcomes and there is an attempt to visually match them by appearance and other traits like pair-object separation. We hope that these results will be a basis for many more researches or reinterpretations of prior publications.

Morphology

There have been many salient nuances observed during these forays into the massive data expanses which further the influence of evidential, anecdotal observations. As in any attempt to delineate novel interpretations of astronomical phenomena we encountered a barrage of new terms to describe these systems. To name a few: wh.dots (white/color compact, stellate emergent or fission object,) umbilicates (Ambartsumian's Knots or small compact objects ugriz r-values in the range 18-19 found with fission pairs,) maple seeds (twinned 'tadpoles',) clam shells (clones resulting from 'binary' fission,) mirrors (similar sized clam shells oriented edge-on and face-on,) minimes (C1 smaller version of P1,) emergent (multi-core systems in common 'halo',) cometoid, ringlet or flung object (an object at the terminus of an arm or 'projected' from an object's arm or core,) dGBs (system with P1 and smaller 'blue' C1 and C2,) GV ("green valley" MTG, red ETG and blue LTG pair,) and 3Ms (dGBs or C1 with a strong Oiii spectrum peak.)

Figure 2. Emergent systems {fig01_030emergent}

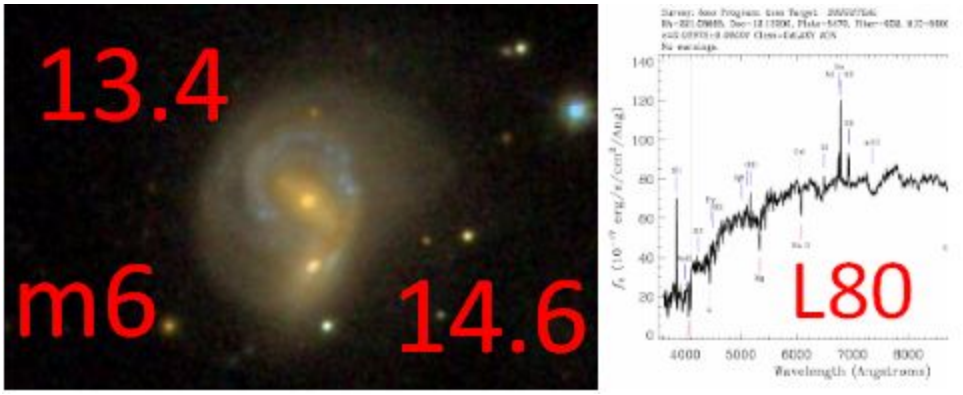

P1 SB AGN and emergent C1 'minime' with trailing star-forming and dust lane 'trains' revealing the 'dustory,' dust history shared during the emergent process.

14.67 14.30 z.029064 1237662636904022101 C1 12.81"
13.44 13.02 z.030268 1237662636904022099 P1

{fig02_063emergent}

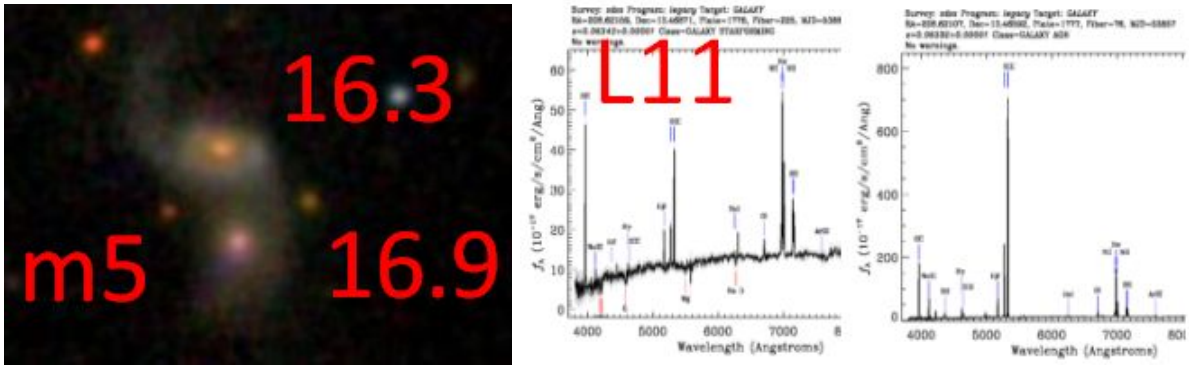

P1 S star-forming 3M (strong Oii, Oiii and Ha) and C1 compact AGN

16.99 16.47 z.06332 1237662529526890706 C1 10.63” XrayS
16.31 15.85 z.06343 1237662529526890705 P1 L11

There are also designations to describe the shared attributes of objects in a system. These all have the suffix “-DNA.” Prefixes include: spec(tra)-, morph(ology)-, size- (fig 2,) broadline-, AGN-, SFing- (star-forming,) Sbst- (star-burst,) dustlane-, and kinetic- (Radio and/or Xray sources.) The most prominent is spec-DNA which confirms our theoretical model of shared chemical composition which would not be the case if the objects were randomly associated.

Figure 3. Morphology and size taxonomy (morph-DNA)

{fig03_taxonomy}

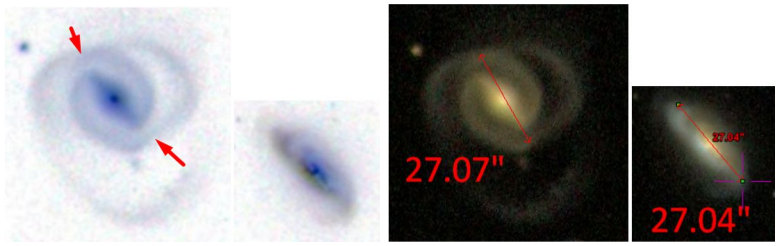

14.88 14.53 z.0279 1237657775007531270 C1 1.817’
14.34 13.94 z.0279 1237657775007531233 P1

The result of fission is expressed as a gamut of possibilities. Most conform to a pattern that results in a pair with an object that is smaller and 'bluer.' We use the designation P1 or p1 to represent the ‘proximal’ object of the pair. The lesser object is the ‘closest’ designated C1 or c1. The fission ‘child’ objects can range from the size of Minkowski Objects (Croft et al. 2006) to a 'mini-me' version of its P1 with degrees of similar ('*-DNA') traits. Moreover there is a set of paired-object systems that are not so neatly divided by size disparity and those ‘clone’-types are nevertheless still considered emergent and fission systems. The clone- and mirror-type systems will be analyzed elsewhere. Also, the additional 'children' of 'family' systems will be analyzed elsewhere. It should be noted that there is a unique system-type that entertains two or multiple 'children' in the family. Our best efforts went into selecting only paired-object systems and those closest, data-driven pairs from families. Using random pairs allowed us to avoid any particular subset selection in the analysis . We gleaned more pairs from new data to supplement the appendix.

Analysis

Analyzed herein are the putative binary pairings chosen from pairs or the nearest data-driven pair of an object family. Moreover, an unary, precursor object splits into a multi-object system with two or more resulting independent objects. Those objects contributed to an analysis of systems with ugriz-r categories ranging from blue pairs to green pairs and red pairs. The term “green” is from references (Wong et al. 2011 and Schawinski et al. 2015) to an intermediate object type positioned, in age, between the youngest ‘blue’ objects and the oldest ‘red’ objects. In Table 1 the systems were first enumerated across 3 redshift ranges by the green pairs and the composited blue and red pairs. The blue and red systems were then partitioned to demonstrate their types. Together the categories, across redshifts, show uniform fission activity. These results should be enhanced considerably with a larger pool of paired-object systems.

Table 1. Fission Systems in Redshift Groups

Fission Types	Z LT 0.05	Z 0.05-0.08	Z GT 0.08
RB pair	173	47	15
BB RR pairs	402	114	39

BB RR pairs	Z LT 0.05	Z 0.05-0.08	Z GT 0.08
BB system	206	59	20
RR system	196	55	19

Notes.

These analyses were run using SAS Studio.

With the encouraging results from Table 1 we then examined the presumptive modulation of the ugriz r-value occurring with the distance between the system objects. Here in Table 2 we find that the r-values lessen (get 'redder') with increased distance of P1 to C1 indicating a relationship where C1 'ages' after fission. At greater redshift the object gap distances are greater than the same gap at a lower redshift. This analysis will be rerun within redshifts at higher redshifts with larger sets of observations.
In the appendix there are examples of C1 possibly contributing to another object, or C1', after a primary fission event. Also, a C1 object may travel with a C2 companion from an initial fission. At this early stage of examining paired-object systems it is highly speculative to suggest how many objects constituted any particular fission system at onset.

Table 2. Same Redshift Systems Reddening by Redshift Groups

Gap distance	Z LT 0.05	Z 0.05-0.08	Z GT 0.08
GE 60 sec LT 60 sec	15.13 50 obs 15.75 38 obs	15.96 8 obs 16.97 30 obs	16.92 3 obs 16.60 13 obs

Notes.
The restriction imposed on the systems to be same-redshift reduced the number of observations. The original data has fewer high-Z mainly due to lack of morphological classification selection an excess of LTGs or late-type galaxies. Also, consider that the gaps distances are physically greater at higher redshifts. The appendix has objects from the analysis (for the type rdif~2) and supplemental pairs to exhibit three pairs for each of the redshifts .01-.13.

Conclusion

Efforts, mainly morphological, have been presented to support the theory of emergent fission systems. By collecting and analyzing random paired-object systems we have constructed a data-driven selection process to demonstrate that galaxies (objects) can be formed from primordial anlage which transform to emergent systems and create a plethora of new multi-object systems. Zwicki mentioned “post-eruptive” morphological formations and Arp has an Atlas of “Peculiar Galaxies.” Among recent reports is one from SISSA “… elliptical galaxies cannot have formed through the merging of other galaxies … This means that the formation of elliptical galaxies occurs through internal, in situ processes of star formation (Mancuso 2016.)”

Also, ”We show that for most present-day galaxies, the 0.4--22 micron SED fits can exquisitely predict the fluxes measured by Herschel at much longer wavelengths. Our analysis also illustrates that the majority of stars in the present-day universe are formed in luminous galaxies (~{L}^*^) in and around the "green valley" of the color-luminosity plane. We make publicly available the matched photometry catalog and SED modeling results (Chang et al., 2015.)”

And from the recent MaNGA studies another note, “Recent studies argue that local galaxies must migrate rapidly (within a Gyr) from the ‘blue cloud’ to the ‘red sequence’ due to the scarcity of galaxies within the intervening parameter space (occasionally dubbed the ‘green valley’; (e.g. Schawinski et al. 2007.) Therefore, valuable insights into galaxy evolution can be obtained by studying galaxies that appear to have intermediate properties and may be in the act of transitioning between the two main galaxy populations (Wong 2011.)” Without a theory of emergent and fission systems there is not going to be a plausible answer to the merger hypothesis.

Footnotes

1 Emergent Gravity and the Dark Universe
https://arxiv.org/pdf/1611.02269v2.pdf

2 These terms should not be confused with similar terms used in SDSS.
http://www.sdss.org/dr12/imaging/imaging_basics/

3 Arps “Galaxies with the appearance of fission.”
https://en.wikipedia.org/wiki/Atlas_of_Peculiar_Galaxies#Galaxies_with_the_appearance_of_fission

4 NED classification types.
http://ned.ipac.caltech.edu/forms/OBJatt.html
http://ned.ipac.caltech.edu/cgi-bin/INFatt?dom=M&id=2812 “merger” type

References

Chang *et al.* 2015 http://iopscience.iop.org/article/10.1088/0067-0049/219/1/8/meta

Croft *et al.* 2006 https://arxiv.org/pdf/astro-ph/0604557v1.pdf

Mancuso 2016 http://www.sciencenewsline.com/news/20160601184300 28.html

Schawinski *et al.* 2007 http://mnras.oxfordjournals.org/content/382/4/1415.full

Schawinski *et al.* 2015 http://adsabs.harvard.edu/abs/2014MNRAS.440..889S

Wong *et al.* 2011 http://mnras.oxfordjournals.org/content/420/2/1684.full

Zwicky *et al.* 1971 http://adsabs.harvard.edu/abs/1971cscg.book.....Z

Appendix

{Exemplar Analogs across redshifts z 0.010 - z 0.130}

Note: "m" is denoting the zoom magnification in the SDSS skyserver viewer. The values in images are ugriz r-values. Values in spectra are 'peak' F-lambdas near Ha. Ordinal designations in the spectra are "c" (child type) or "p" (parent type.) The object's data has ugriz-r, ugriz-i, redshift, object ID, object-pair index key, object system type and distance between objects. Some objects may not have a spectrum. Pairs from the analysis are listed as they were output from a sort program.

The appendix has the set of object-pairs with rdif~2 from the analysis and supplemental object-pairs to fill gaps in the sequence across redshifts.

{fig04_010607}

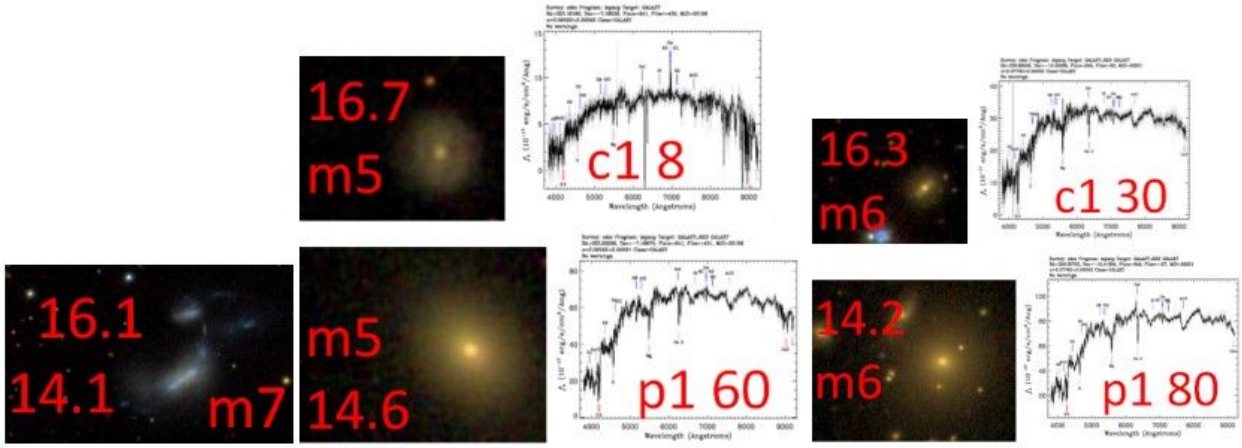

Obs#615 z = 0.0109, Obs#616 z = 0.0606 and Obs#617 z = 0.0776

{Additional z 0.01 Exemplar Analogs across redshifts}
{fig05_appendix01}

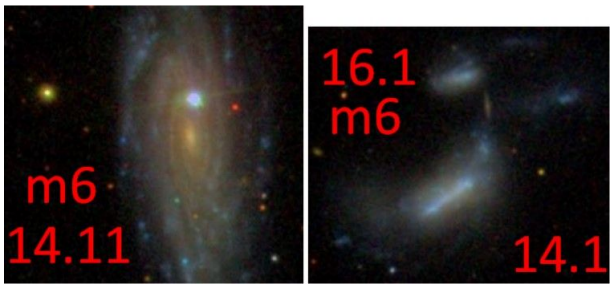

16.19 16.11 z.0111 1237674459874591027 1237674459874591026 C1 47.32”
14.10 13.97 z.0109 1237674459874591026 1237674459874591026 P1 And …
14.10 13.97 z.0109 1237674459874591026 1237673708792250464 P1 14.01’
14.11 13.60 z.0110 1237673708792250464 1237673708792250464 P0
{fig06_exemplar013p1c1}

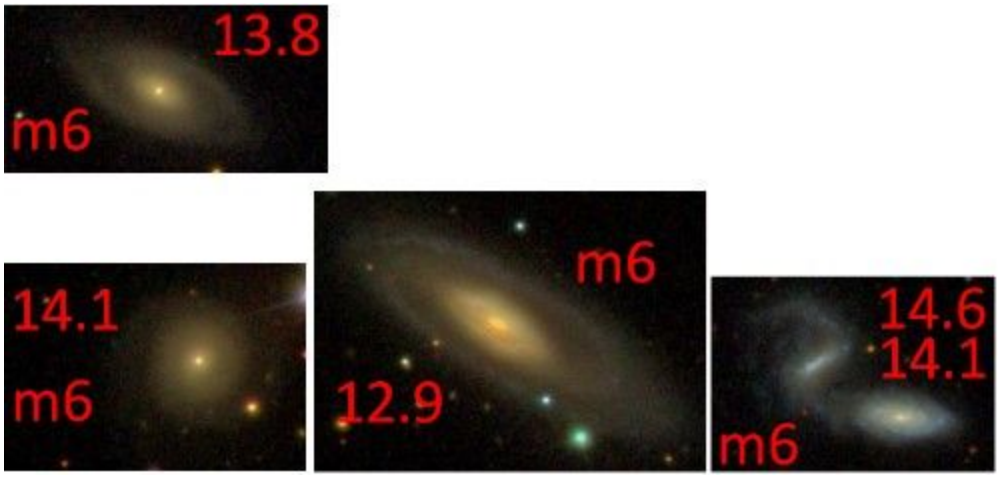

14.67 14.47 z.01376 1237653665249493167 1237653665249493166 C1 34.92”
14.16 13.94 z.01377 1237653665249493166 1237653665249493166 P1 And …
14.67 14.47 z.01376 1237653665249493167 1237653665249624220 C0 18.93’
12.91 12.38 z.01368 1237653665249624220 1237653665249624220 P0
13.85 13.47 z.01307 1237653622837084592

{Additional z 0.01 Exemplar Analogs across redshifts}
{fig07_exemplar018p1c1}

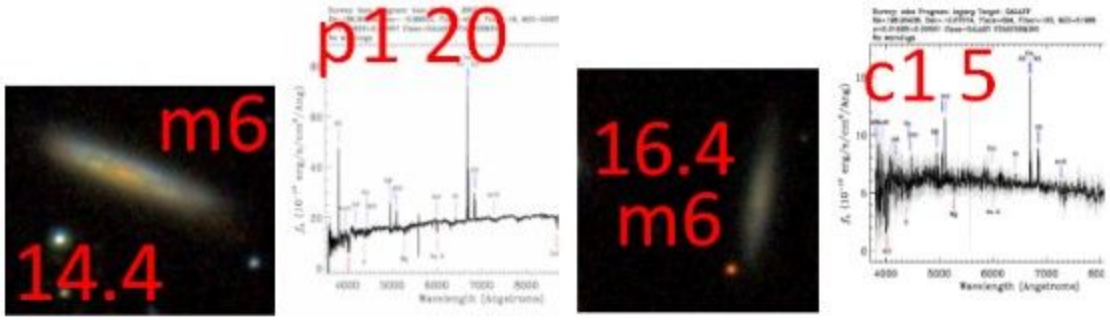

16.45 16.19 z.01826 1237648720701292666 1237648720164421894 C1 17.71'
14.45 14.11 z.01820 1237648720164421894 1237648720164421894 P1
{fig08_exemplar019c1}

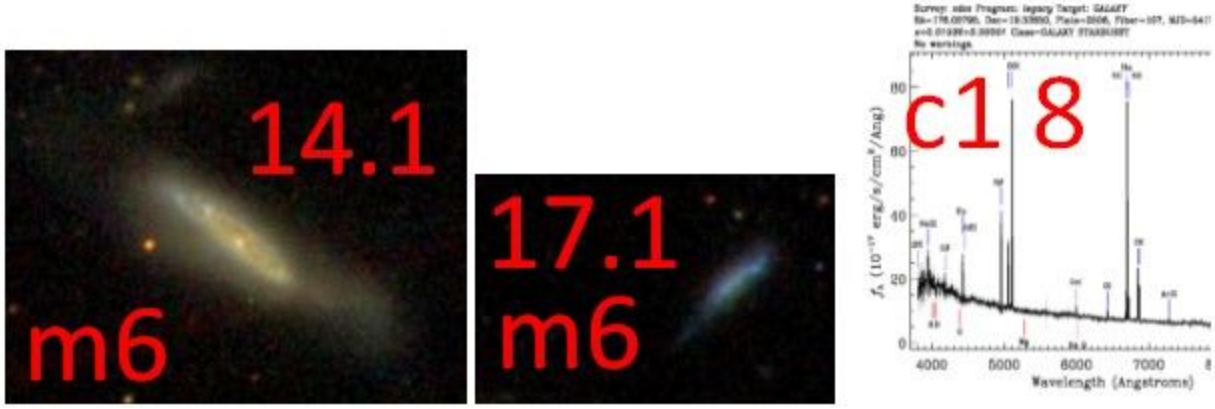

17.37 17.27 z.0193 1237667914879795415 1237668293375885373 C1 11.47'
14.17 13.82 z.0182 1237668293375885373 1237668293375885373 P1
{fig09_exemplar019p1c1}

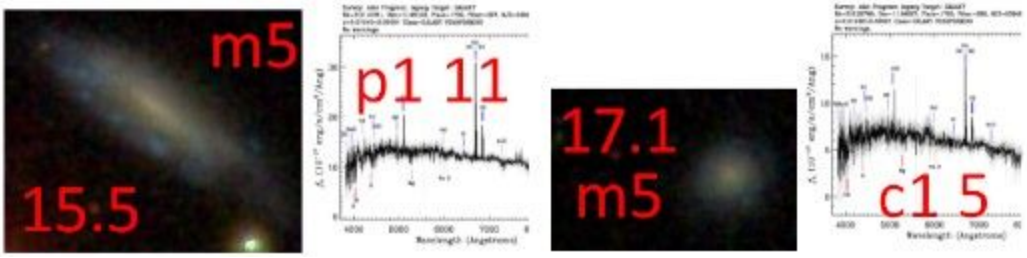

17.10 16.93 z.0193 1237661950803050806 1237661950803050536 C1 4.724'
15.57 15.29 z.0194 1237661950803050536 1237661950803050536 P1

{Additional z 0.06 Exemplar Analogs across redshifts}
{fig10_exemplar065p1c1}

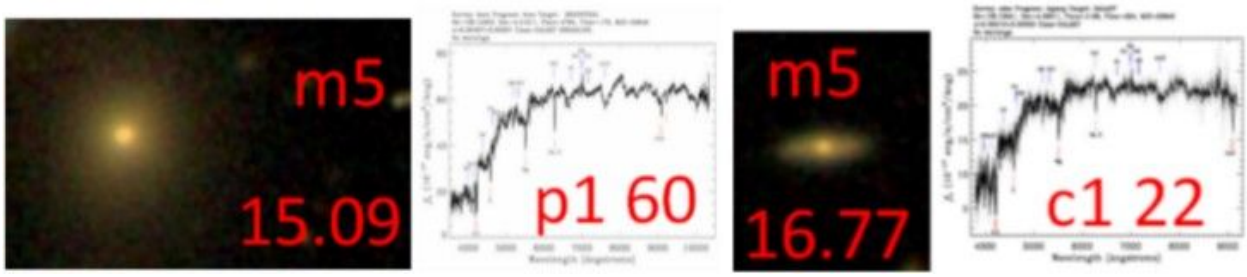

16.77 16.34 z.0651 1237658424076796258 1237658424076796002 C1 1.551’
15.09 14.64 z.0646 1237658424076796002 1237658424076796002 P1
{fig11_exemplar063p1c1}

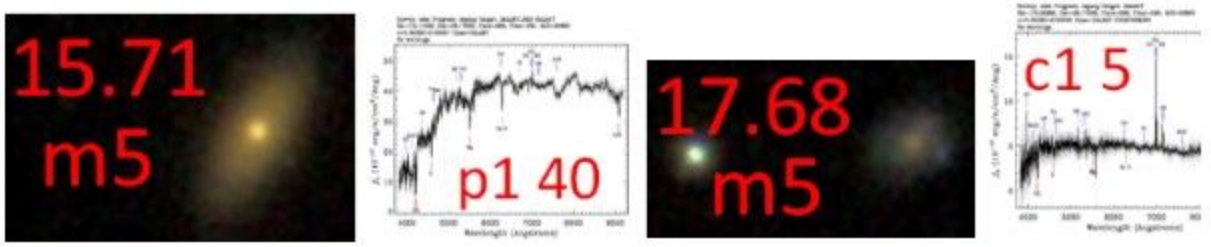

17.68 17.37 z.0638 1237657608566735487 1237657608566800801 C1 4.197’
15.71 15.27 z.0638 1237657608566800801 1237657608566800801 P1
{fig12_exemplar064p1c1}

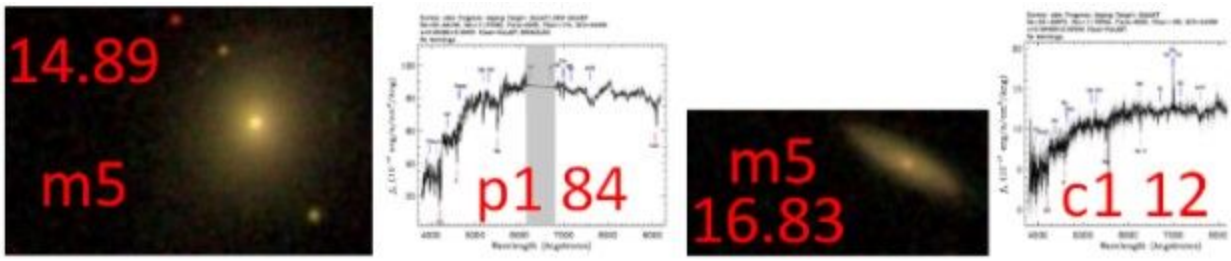

16.83 16.40 z.0640 1237668272452075945 1237668272452075924 C1 3.084’
14.89 14.50 z.0639 1237668272452075924 1237668272452075924 P1

{Additional z 0.07 Exemplar Analogs across redshifts}
{fig13_exemplar073p1c1}

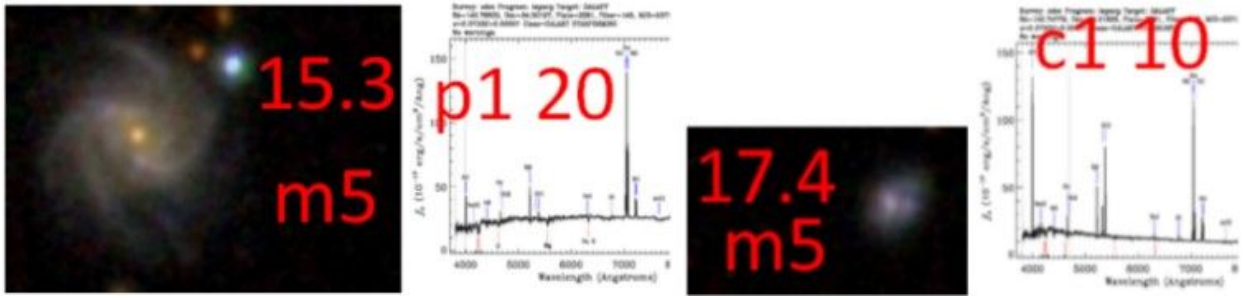

17.42 17.13 z.0730 1237667141793546406 1237667141793546276 C1 1.427’
15.32 14.97 z.0733 1237667141793546276 1237667141793546276 P1
{fig14_exemplar076p1c1}

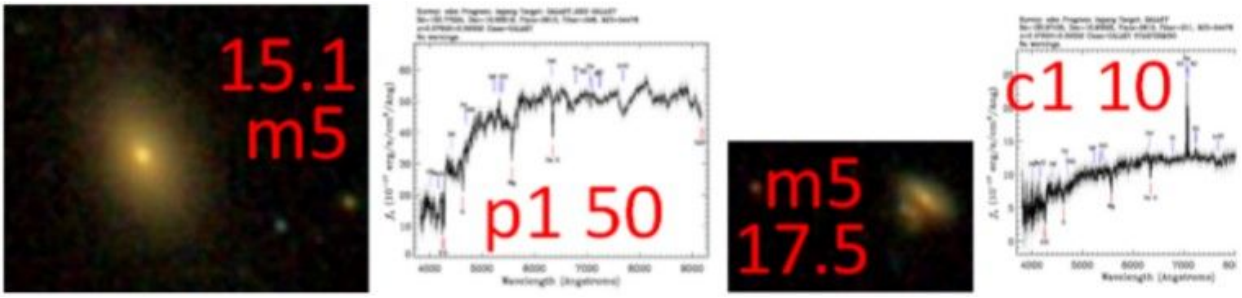

17.52 17.07 z.0760 1237668296593047689 1237668296592982163 C1 8.173’
15.13 14.68 z.0760 1237668296592982163 1237668296592982163 P1
{fig15_exemplar073c1p1}

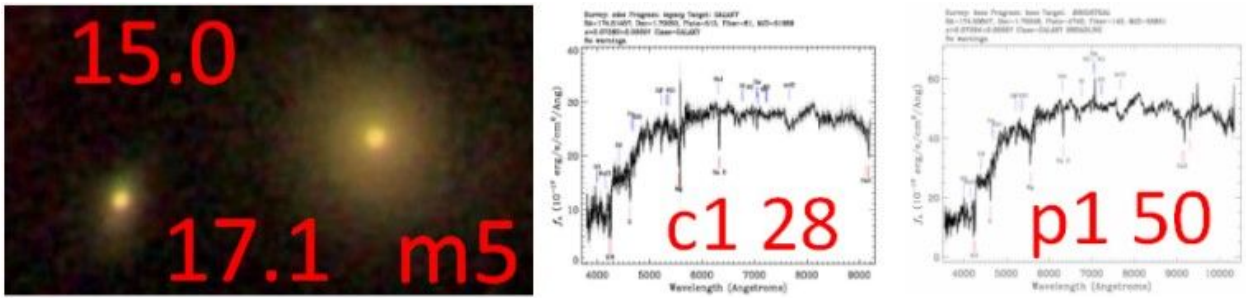

17.17 17.11 z.0738 1237651752934178943 1237651752934178942 C1 30.01"
15.03 14.58 z.0739 1237651752934178942 1237651752934178942 P1

{Additional z 0.02 Exemplar Analogs across redshifts}
{fig16_latex020305}

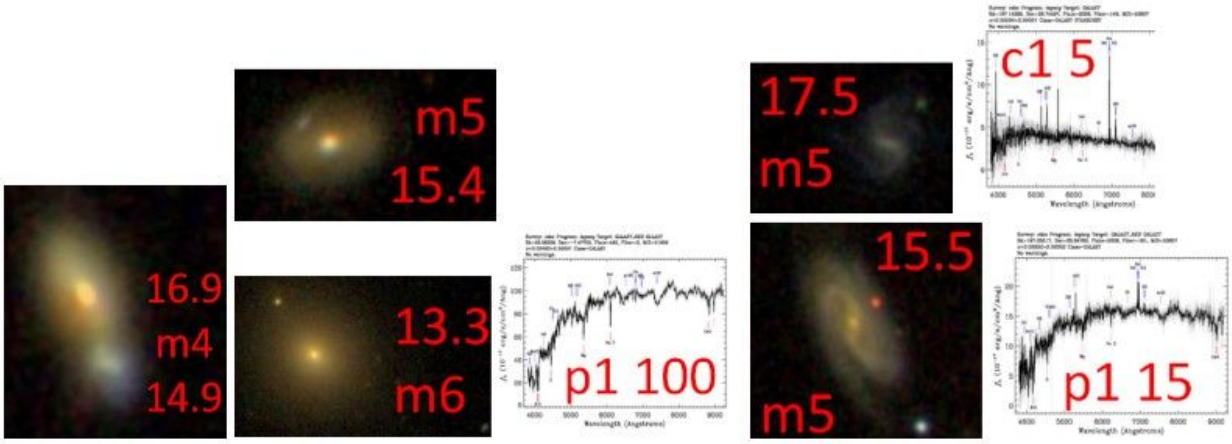

Obs#608 z = 0.0277, Obs#612 z = 0.0349, Obs#613 z = 0.0565

{Additional z 0.02 Exemplar Analogs across redshifts}
{fig17_exemplar025p1c1}

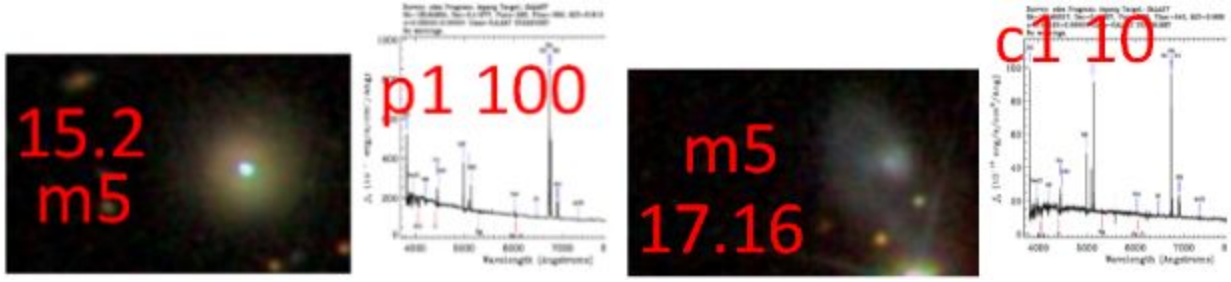

17.16 17.06 z.02523 1237674650997882950 1237648721763041373 C1 2.999’
15.22 14.99 z.02503 1237648721763041373 1237648721763041373 P1
{fig18_exemplar022p1c1}

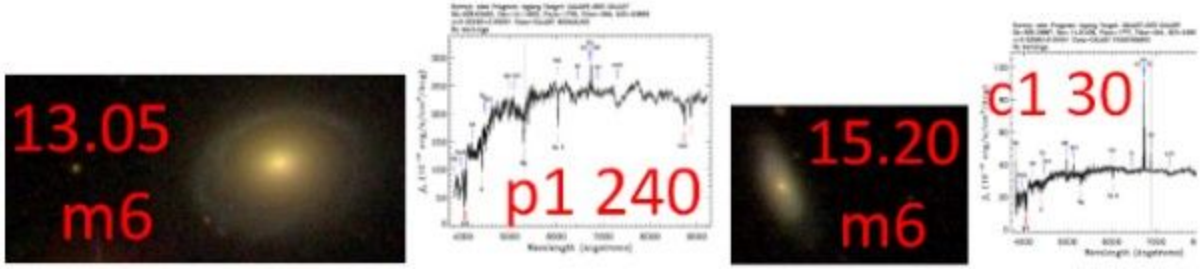

15.20 14.84 z.0226 1237662530063564997 1237664291011952667 C1 10.83’
13.05 12.67 z.0226 1237664291011952667 1237664291011952667 P1
{fig19_exemplar023p1c1}

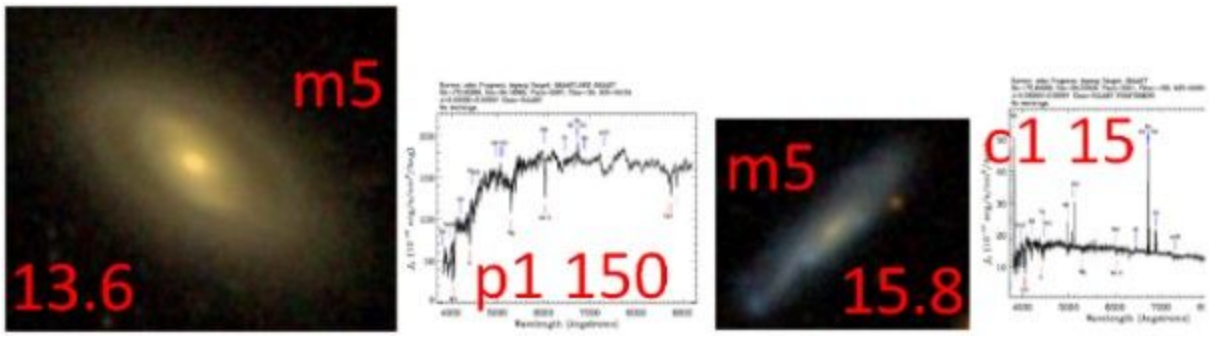

15.87 15.69 z.0226 1237667911125172378 1237667911125172234 C1 5.683’
13.63 13.24 z.0233 1237667911125172234 1237667911125172234 P1

{Additional z 0.03 Exemplar Analogs across redshifts}
{fig20_exemplar037p1c1}

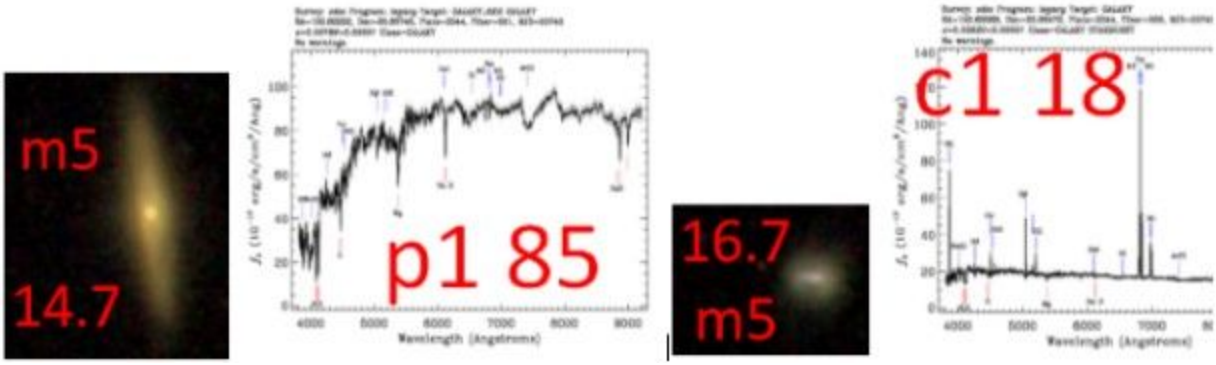

16.78 16.48 z.0382 1237667211589779623 1237667211589845183 C1 7.665'
14.74 14.33 z.0378 1237667211589845183 1237667211589845183 P1
{fig21_exemplar036p1c1}

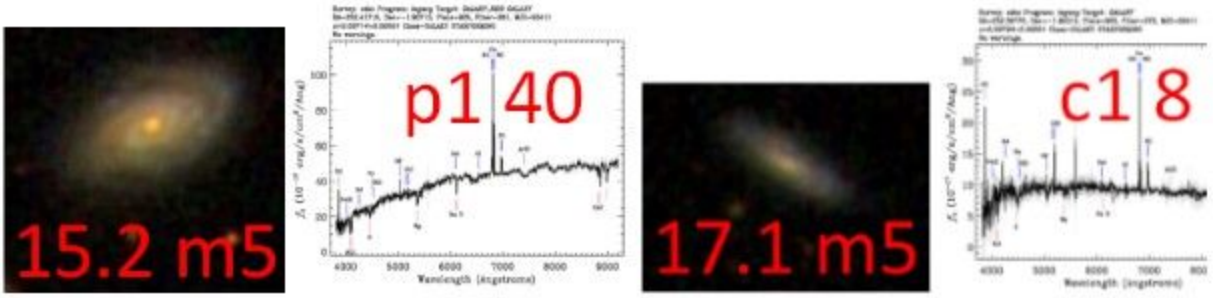

17.10 16.78 z.0372 1237655691944722716 1237655691944722737 C1 1.506'
15.22 14.78 z.0371 1237655691944722737 1237655691944722737 P1
{fig22_exemplar034p1c1}

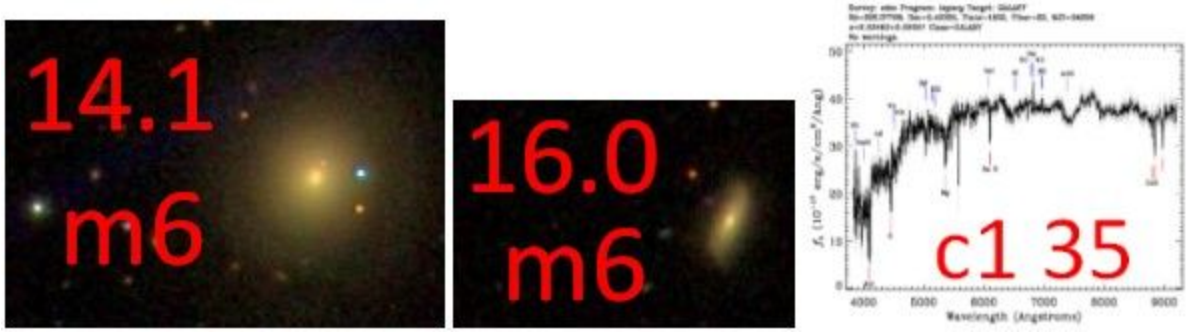

16.02 15.63 z.0346 1237662267537424674 1237662267537424497 C1 1.713'
14.17 13.75 z.0347 1237662267537424497 1237662267537424497 P1

{Additional z 0.05 Exemplar Analogs across redshifts}
{fig23_exemplar050p1c1}

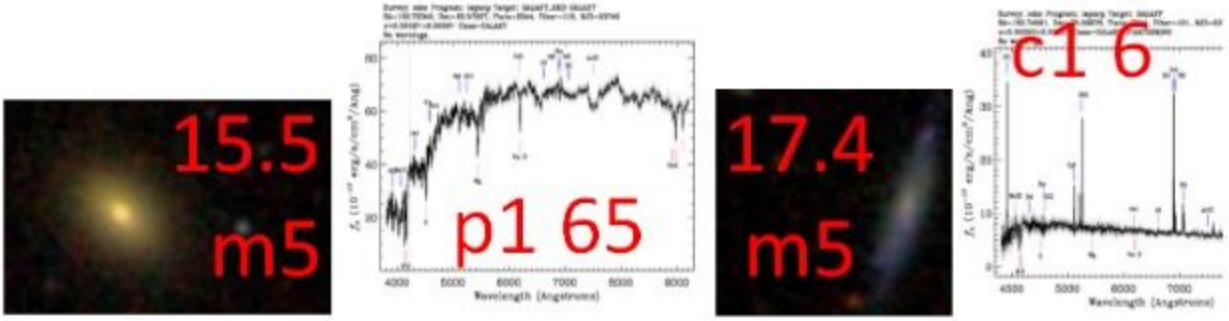

17.40 17.19 z.0505 1237667211589845100 1237667211589779628 C1 2.055’
15.55 15.14 z.0502 1237667211589779628 1237667211589779628 P1
{fig24_exemplar053p1c1}

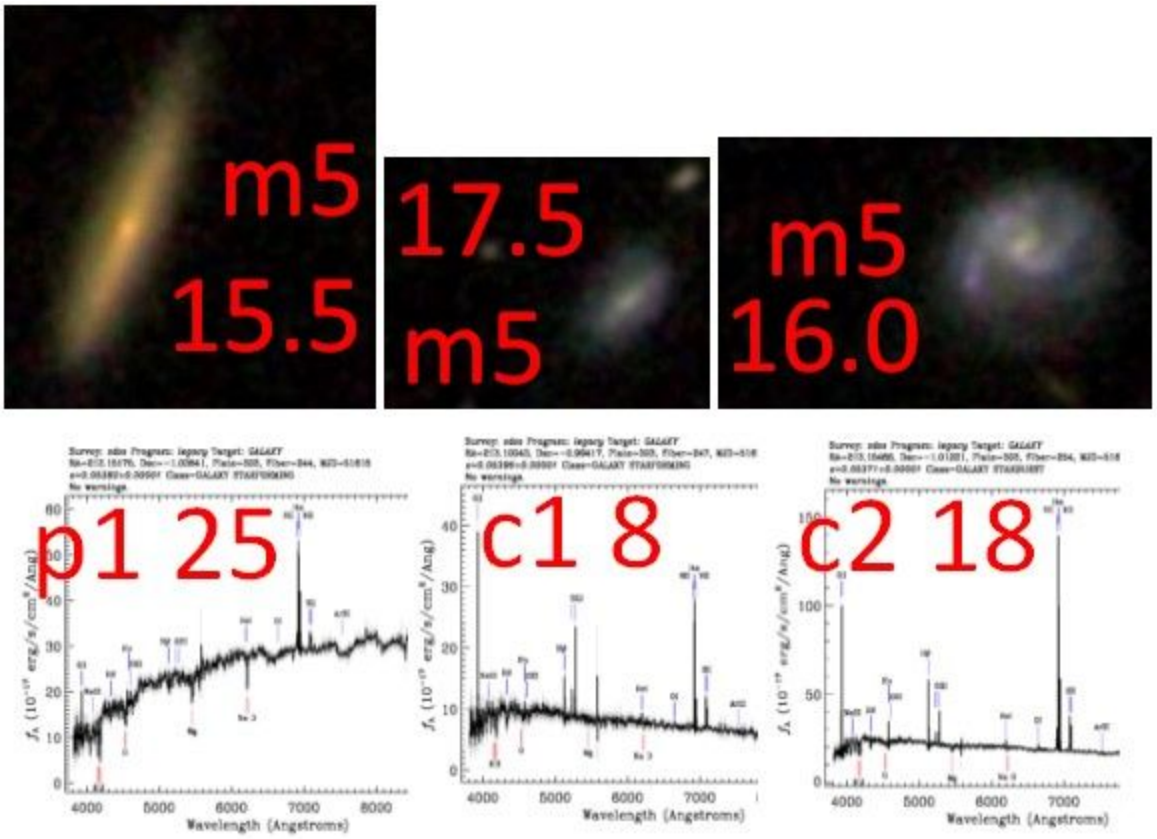

16.03 15.76 z.0537 1237674602679632071 1237674602679632087 C2 1.464’
17.59 17.37 z.0539 1237674602679632024 1237674602679632087 C1 3.993’
15.59 15.11 z.0538 1237674602679632087 1237674602679632087 P1

{Additional z 0.05 Exemplar Analogs across redshifts}
{fig25_exemplar053c1p1}

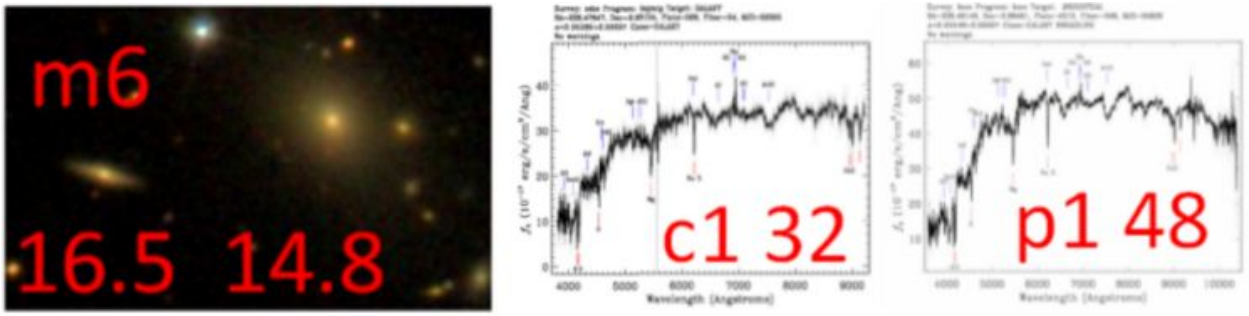

16.52 16.06 z.05385 1237655470208647510 1237655470208647275 C1 55.39”
14.80 14.36 z.05548 1237655470208647275 1237655470208647275 P1
{fig26_exemplar054p1c1}

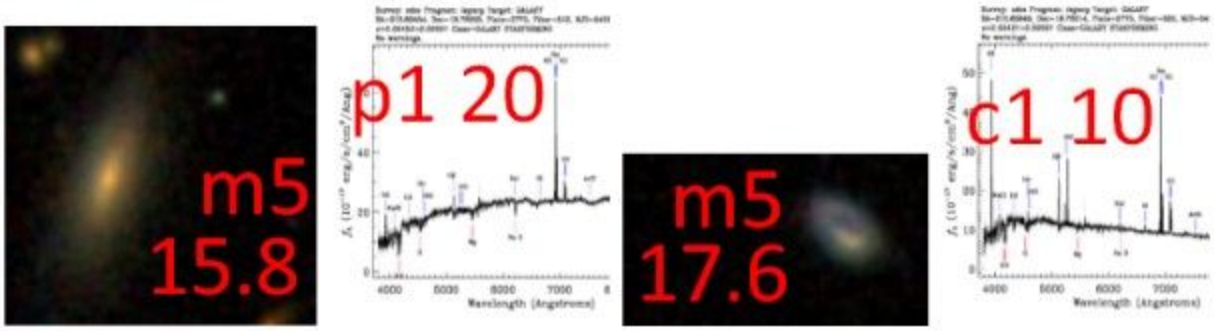

17.66 17.41 z.0545 1237667782847299765 1237667782847299652 C1 2.143’
15.85 15.40 z.0545 1237667782847299652 1237667782847299652 P1

{Additional z 0.04 Exemplar Analogs across redshifts}
{fig27_exemplar619}

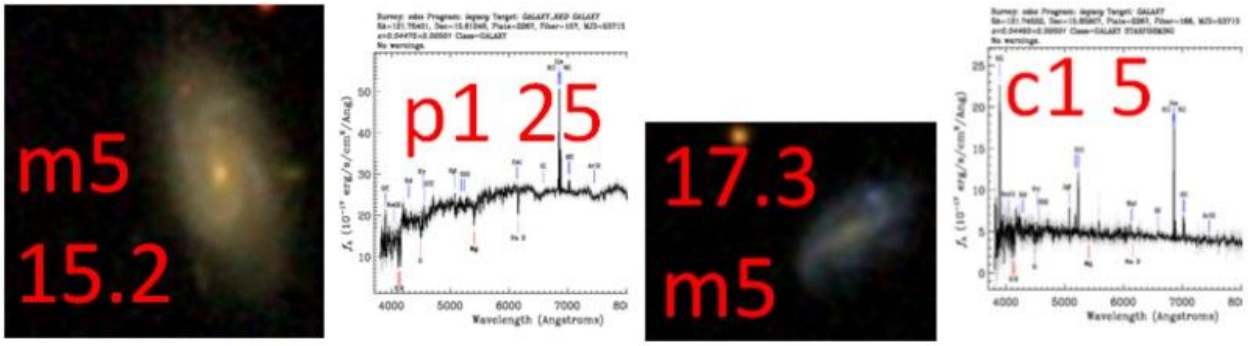

Obs#619 z = 0.0447
17.35 17.19 .0446 1237667107961307583 1237667107961307571 C1 2.839’
15.25 14.86 .0447 1237667107961307571 1237667107961307571 P1
{fig28_exemplar048p1c1}

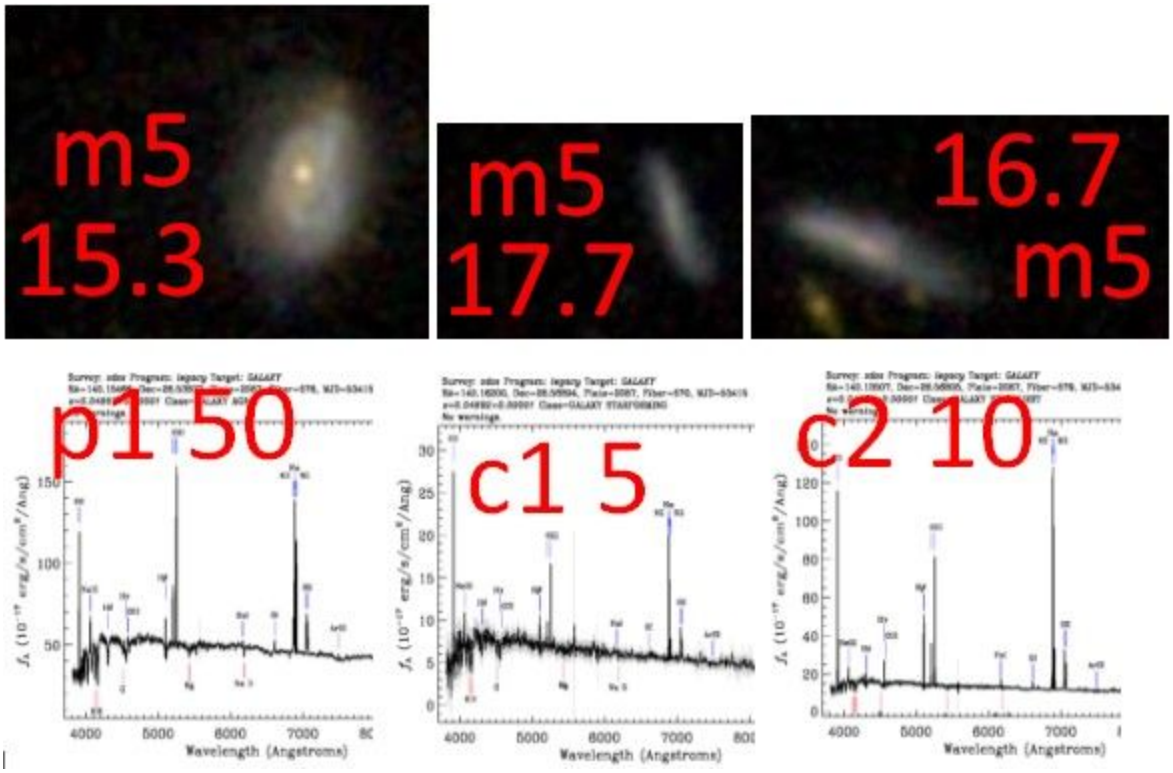

16.73 16.43 z.0490 1237665128526839908 1237665128526839916 C2 2.073’
17.78 17.54 z.0489 1237665128526839946 1237665128526839916 C1 3.076’
15.36 15.07 z.0485 1237665128526839916 1237665128526839916 P1

{Additional z 0.04 Exemplar Analogs across redshifts}
{fig29_exemplar046p1c1}

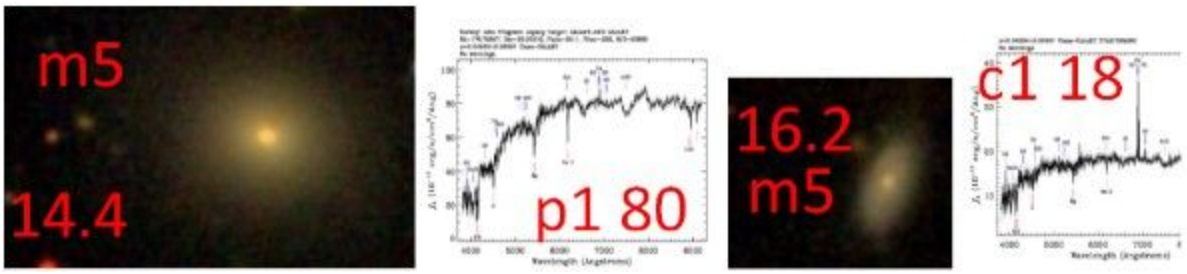

16.27 15.92 z.0493 1237667917027606533 1237667917027606649 C1 1.782’
14.41 14.03 z.0485 1237667917027606649 1237667917027606649 P1
{fig30_exemplar044p1c1}

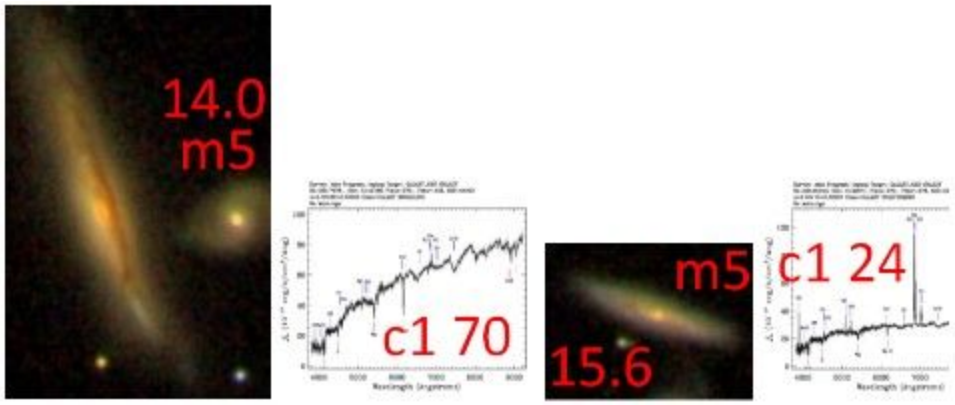

15.67 15.24 z.0441 1237668332029935885 1237668332029935843 C1 1.834’
14.05 13.49 z.0436 1237668332029935843 1237668332029935843 P1
{fig31_exemplar042p1c1}

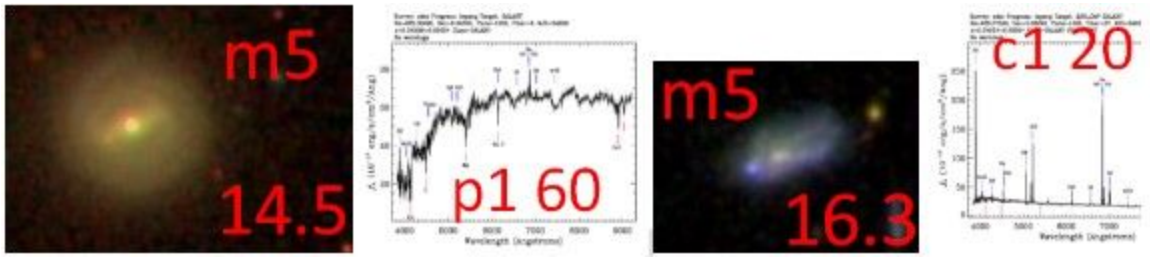

16.32 16.09 z.0425 1237662267537424425 1237662267000553801 C1 13.36’
14.54 14.15 z.0432 1237662267000553801 1237662267000553801 P1

{Additional z 0.08 Exemplar Analogs across redshifts}
{fig32_exemplar085p1c1}

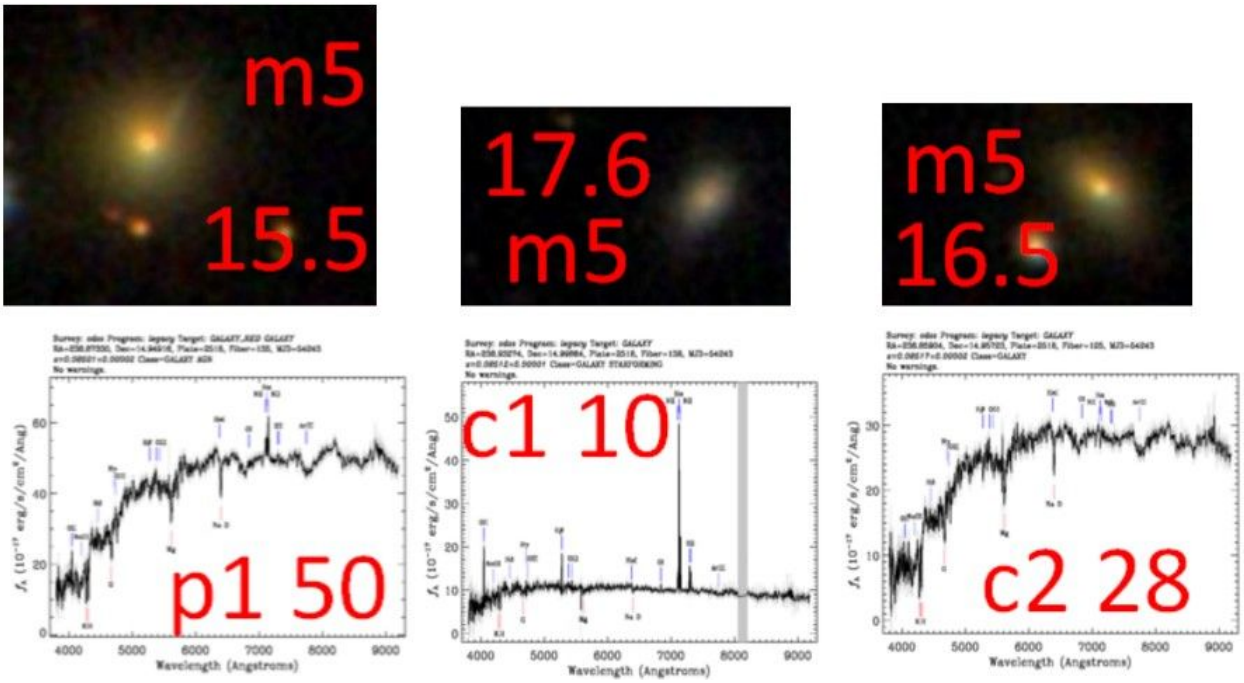

16.51 16.07 z.0851 1237665565006168400 1237665565006168232 C2 56.36”
17.60 17.23 z.0851 1237665565006168465 1237665565006168232 C1 4.541’
15.59 15.12 z.0850 1237665565006168232 1237665565006168232 P1
{fig33_exemplar086p1c1}

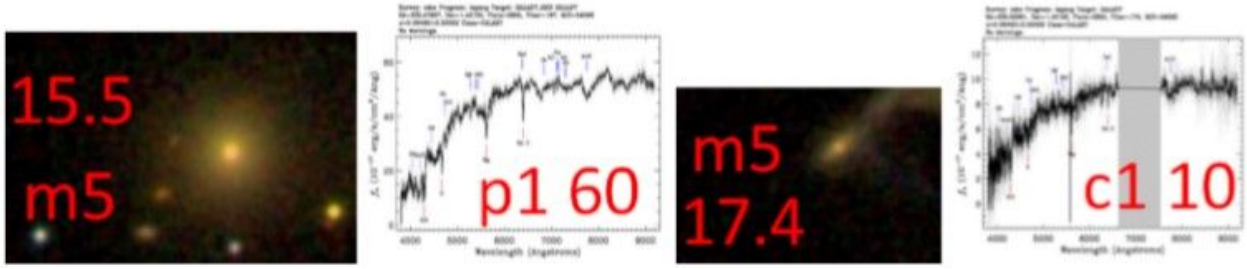

15.25 14.78 z.0848 1237651736318116090 1237651736318116174 C1 2.44’
17.41 16.93 z.0846 1237651736318116174 1237651736318116174 P1

{Additional z 0.08 Exemplar Analogs across redshifts}
{fig34_exemplar081p1c1}

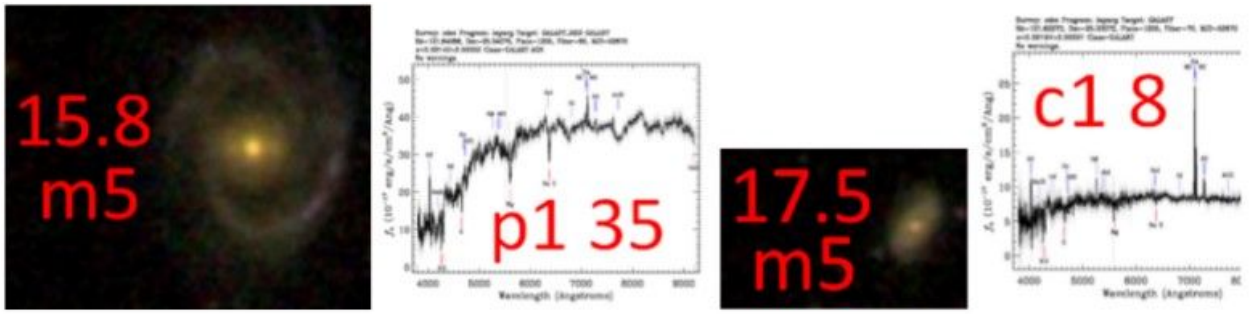

17.59 17.20 z.0816 1237660561895195039 1237660561895195063 C1 1.139’
15.88 15.44 z.0814 1237660561895195063 1237660561895195063 P1

{Additional z 0.09 Exemplar Analogs across redshifts}
{fig35_exemplar090p1c1}

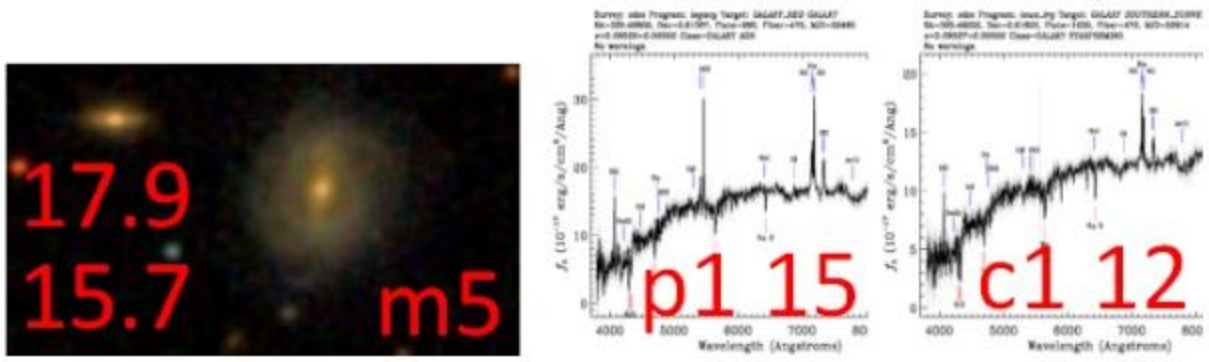

17.96 17.41 z.0902 1237656238472036912 1237656238472036897 C1 24.51”
15.78 15.35 z.0902 1237656238472036897 1237656238472036897 P1
{fig36_exemplar093p1c1}

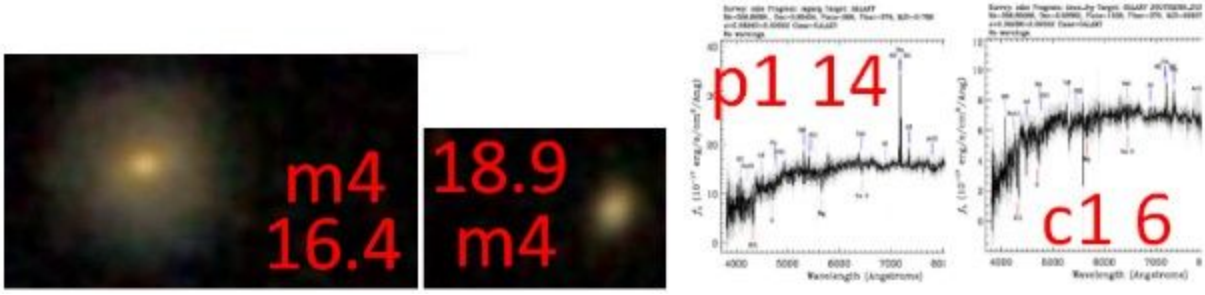

18.90 18.50 z.0929 1237663278463254729 1237663278463254738 C1 32.06”
16.43 16.04 z.0926 1237663278463254738 1237663278463254738 P1
{fig37_exemplar098p1c1}

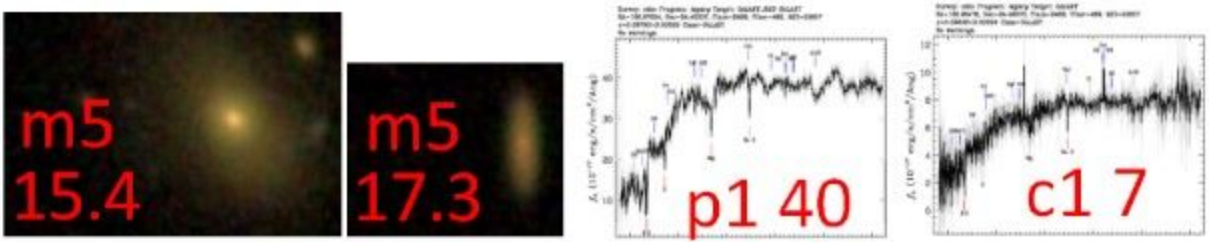

17.37 16.90 z.0984 1237667912196685984 1237667912196685991 C1 1.241’
15.44 15.03 z.0979 1237667912196685991 1237667912196685991 P1

{Additional z 0.1 Exemplar Analogs across redshifts}
{fig38_exemplar100p1c1}

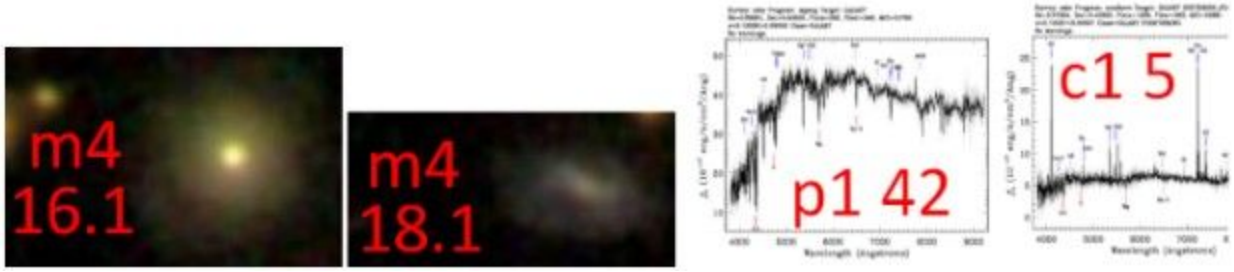

18.14 17.87 z .1002 1237663277928153273 1237663277928153250 C1 37.54"
16.18 15.87 z .1003 1237663277928153250 1237663277928153250 P1
{fig39_exemplar103p1c1}

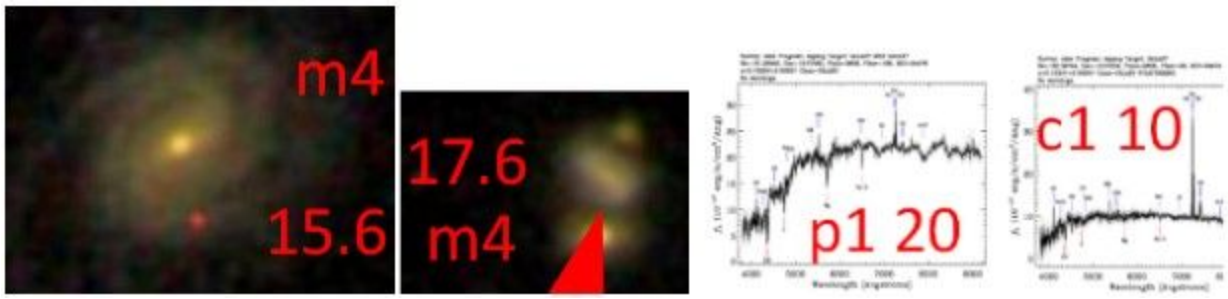

17.64 17.23 z.1034 1237668297666003121 1237668297666003072 C1 8.037'
15.62 15.20 z.1020 1237668297666003072 1237668297666003072 P1
{fig40_exemplar119p1c1}

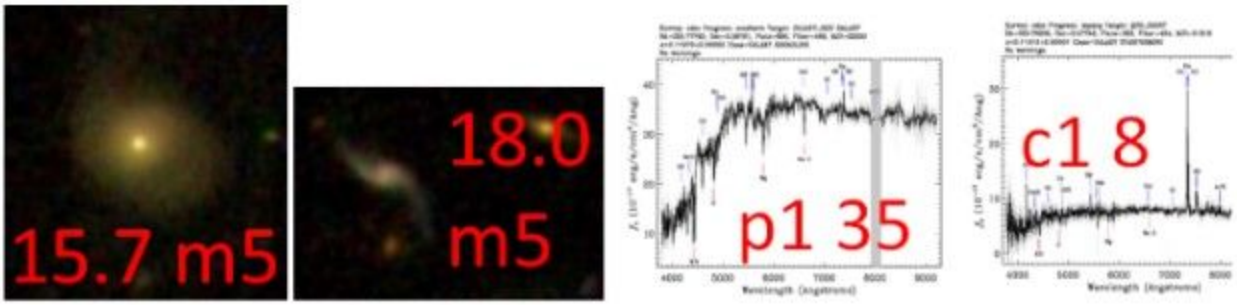

18.09 17.67 z.1191 1237663277923696846 1237663277923696815 C1 38.38"
15.75 15.33 z.1197 1237663277923696815 1237663277923696815 P1